



Phosphorus content effect on the magnetoelectric properties of the Ni–P(Ni)/PZT/Ni–P(Ni) cylindrical layered composites



De'an Pan^{a,*}, Jiao Wang^a, Zhijun Zuo^a, Shengen Zhang^a, Bo Liu^a, Alex A. Volinsky^b, Lijie Qiao^a

^a Institute of Advanced Materials and Technology, University of Science and Technology Beijing, Beijing 100083, China

^b Department of Mechanical Engineering, University of South Florida, Tampa, FL 33620, USA

ARTICLE INFO

Article history:

Received 5 June 2014

Accepted 6 July 2014

Available online 14 July 2014

Keywords:

Composite materials

Laminates

Deposition

Magnetic materials

Phosphorus content

ABSTRACT

Ni–P(Ni)/PZT/Ni–P(Ni) cylindrical layered magnetoelectric (ME) composites have been prepared with varying phosphorus content. The axial ME voltage coefficient, $\alpha_{E,A}$, was studied in this paper. The Ni–P/PZT/Ni–P composites show lower optimal magnetic field, $H_{dc,opt}$, along with better linearity of the ME voltage coefficient, compared with the Ni/PZT/Ni composite. These effects may be caused by the high permeability of Ni–P layers. This study helps selecting the appropriate phosphorus content to reduce the magnetic field on the premise of the high ME effect.

© 2014 Elsevier B.V. All rights reserved.

1. Introduction

Multiferroic materials with the coexistence of at least two ferroic orders (ferroelectric, (anti-)ferromagnetic, and ferroelastic) have recently drawn much attention due to their potential applications in multifunctional devices [1,2]. The coupling between the ferromagnetic and ferroelectric orders can lead to the ME effects, defined as an induced dielectric polarization under an applied magnetic field (H), and vice versa [3]. Especially, laminated ME composites made by combining magnetostrictive and piezoelectric layers, have many potential applications, including sensors, actuators and transducers, and have become a popular research topic [4–6].

Giant ME effect in laminated ME composites is an important research topic, capable to meet the practical applications demands. Pan et al. [7,8] have realized the giant ME coupling in the Ni/PZT and Ni/PZT/Ni cylindrical structures by electrodeposition. In line with improving the interfacial bonding and strengthen the coupling between the phases, Bi et al. [9] have successfully prepared Ni/PZT/Ni cylindrical layered ME composites by electroless deposition. Device miniaturization for applications in magnetic sensing and transducers calls for lowering the required $H_{dc,opt}$ by using an alternative magnetostrictive phase [10–12]. Pan et al. [13] found that the required dc magnetic bias can be significantly altered in the Ni–P/PZT/Ni–P cylindrical layered ME composites made by electroless deposition. Based on the above

reports, Ni/PZT/Ni and Ni–P/PZT/Ni–P cylindrical layered ME composites have been prepared by electrodeposition and electroless deposition, respectively. In this work, the effect of phosphorus content on the ME performance in Ni–P(Ni)/PZT/Ni–P(Ni) cylindrical layered magnetoelectric composites was investigated.

2. Experiment

The PZT cylinders with the $\phi 20 \times \phi 18 \times 10$ mm³ dimensions were polarized along the radial direction after electroplating a thin Ni layer on its inside and outside surfaces. The samples were pretreated with supersonic cleaning prior to Ni electroplating. The pretreatment of the electroless Ni–P samples also required the sulfuric acid cathodic activation process. The bath composition and the deposition conditions of Ni electrodeposition and Ni–P electroless deposition are presented in detail elsewhere [8,13]. By adjusting the certain elements of the electroless plating solution, Ni–P alloys with different phosphorus content were obtained. The three samples were designed for this contrast experiment. The detailed schematic of the Ni–P/PZT/Ni–P cylindrical layered composite is shown elsewhere [13].

The final thickness of the inside and the outside coatings was approximately 400 μ m for all the samples. The ME effect of the Ni–P/PZT/Ni–P cylindrical layered composites was obtained in the ME measurement system (supported by Jun Lu, State Key Laboratory of Magnetism, Institute of Physics, Chinese Academy of Sciences, Beijing 100190, China), where constant (H_{DC}) and alternating (δH) magnetic fields were applied in the parallel (axial) mode [13].

* Corresponding author. Tel.: +86 10 82376835; fax: +86 10 62333375.

E-mail address: pandean@mater.ustb.edu.cn (D. Pan).

3. Results and discussion

Fig. 1(a–c) shows the energy dispersive X-ray spectra (EDS) of the Ni layer and Ni–P layers, indicating that no impurities exist and the phosphorus content in the three samples is approximately 0 wt%, 9.78 wt% and 11.36 wt%, respectively. Fig. 1(d) displays the typical X-ray diffraction (XRD) patterns of the three samples. The Ni layer has a sharp (111) peak at $2\theta=45^\circ$, while both Ni–P layers have diffused peaks, corresponding to the amorphous structure, and the higher the phosphorus content, the greater the peak width [14].

Fig. 2 shows the magnetoelectric voltage coefficient, $\alpha_{E,A}$, dependence on the bias magnetic field, H_{DC} , at $f=1$ kHz for the Ni–P(Ni)/PZT/Ni–P(Ni) cylindrical layered composites with various phosphorus content. The $\alpha_{E,A}$ behavior with the bias magnetic field, H_{DC} , is similar for all the samples. With the H_{DC} increase, $\alpha_{E,A}$ has a sharp increase to the maximum value at $H_m=370$ Oe, 80 Oe and 90 Oe, respectively (P content varying from low to high). Then, $\alpha_{E,A}$ decreases rapidly to a near-zero value, since the magnetostrictive phases are saturated. By contrast, the optimal bias magnetic field, $H_{dc,opt}=H_m$, decreases and then increases with the phosphorus content in the Ni–P (Ni) layers.

Fig. 3 shows the frequency dependence of $\alpha_{E,A}$ under the respective optimal magnetic field of the three samples. When the phosphorus content in Ni–P layers is 0%, 9.78% and 11.36%, respectively, the resonance frequencies are 61.2 kHz, 59.8 kHz and 58.6 kHz. As seen in Fig. 3, with the P content increase in the Ni–P layer, resonance frequency is reduced, and the maximum value of $\alpha_{E,A}$ decreases gradually from 6.5–0.6 V/cm Oe. The resonance frequency is associated with the electromechanical resonance [15]. The resonance frequency for the cylindrical layered ME

composites is

$$f_r = \frac{1}{\pi D} \sqrt{\frac{1}{\bar{\rho} \bar{s}_{11}}} \quad (1)$$

The inherent parameters, such as the average density, $\bar{\rho}$, and the equivalent elastic compliance, \bar{s}_{11} , are changed because of the various phosphorus content, thereby leading to different resonant frequencies [16]. Accordingly, the magnetostrictive Ni phase content reduces, causing the weakening of the magnetoelectric coupling effect.

Fig. 4 shows the $\alpha_{E,A}$ dependence on H_{DC} at the respective resonance frequency of the three samples with various phosphorus content. For all samples, $\alpha_{E,A}$ is increasing with H_{DC} until the local maximum value is reached at H_m , and then $\alpha_{E,A}$ subsequently decreases. With further increase of H_{DC} , $\alpha_{E,A}$ increases linearly with H_{DC} between the initial value of the linear region at $H_{DC,i}$ and 5 kOe. Comparing the three composites, the curve of the $\alpha_{E,A}$ dependence on H_{DC} integrally shifts to the left at the resonance frequency with the phosphorus content increase. As seen in Fig. 4, the H_m has the lowest value at 9.78% P, showing the best linearity ($R^2=0.9998$). Besides, its ME effect is overall much better than that of the high P content sample.

The low $H_{dc,opt}$ and the good linear relationship may both be attributed to the high permeability of the Ni–P alloy. High permeability contributes to the concentrated external flux, resulting in stronger magnetic induction B , in turn leading to higher effective piezomagnetic coefficient [11,17]. Ni–P layers have high permeability due to the influence of amorphous nanocrystalline structure. With the increase of phosphorus content, Ni–P alloy will transform from

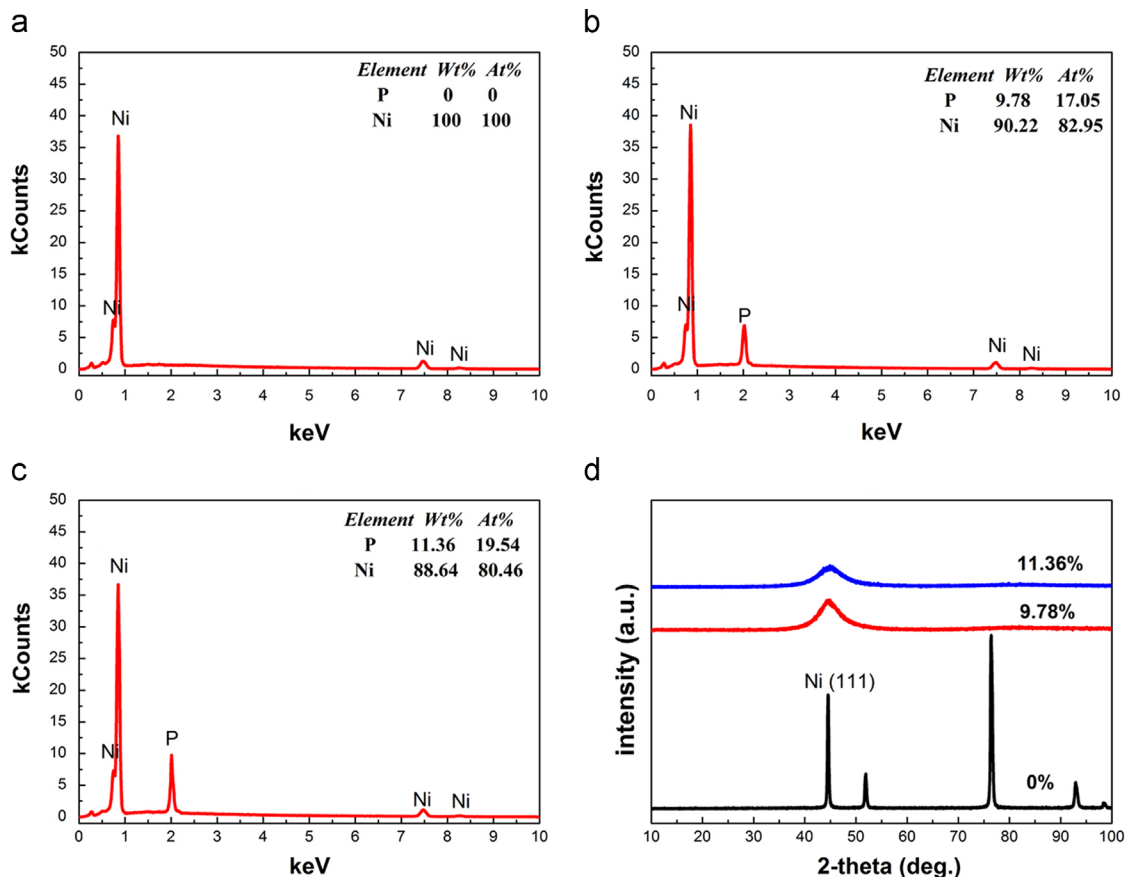


Fig. 1. EDS spectra of: (a) the Ni layer; (b) and (c) Ni–P layers; (d) XRD pattern of the Ni and Ni–P layers with various phosphorus content.

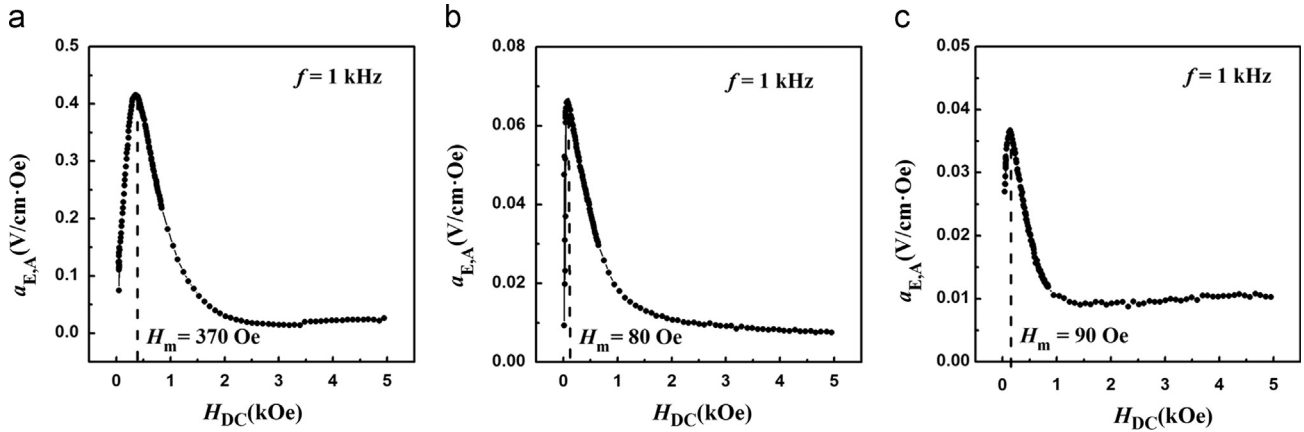


Fig. 2. $\alpha_{E,A}$ dependence on H_{DC} at $f=1$ kHz with various phosphorus contents: (a) 0% P; (b) 9.78% P; (c) 11.36% P.

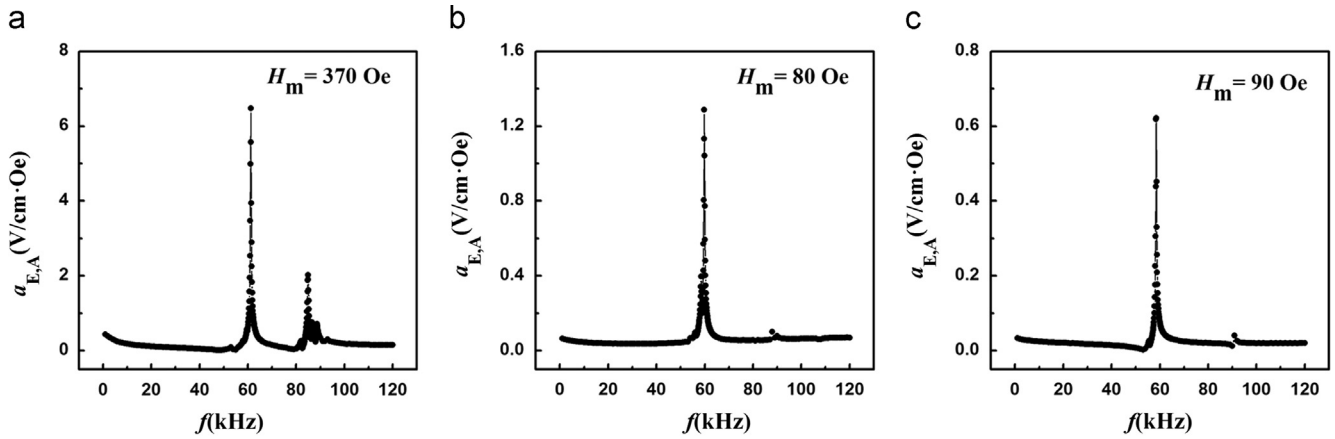


Fig. 3. $\alpha_{E,A}$ AC magnetic field frequency, f , dependence at the respective optimal magnetic field with various phosphorus contents: (a) 0% P; (b) 9.78% P; (c) 11.36% P.

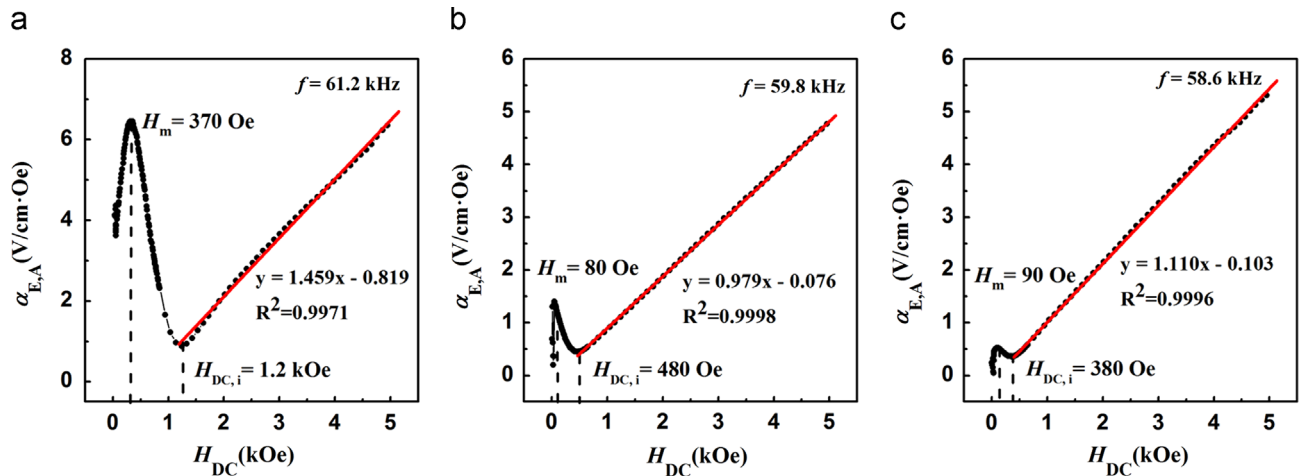


Fig. 4. $\alpha_{E,A}$ dependence on the H_{DC} at the resonance frequency, along with the linear fit: (a) 0% P, (b) 9.78% P, and (c) 11.36% P.

the microcrystalline to the amorphous state [18]. However, since the Ni-P alloy with a very high phosphorus content is fully amorphous, it barely has any magnetic performance, negatively impacting the ME effect [19]. Medium phosphorus content of the Ni-P layer is in the mixed state of amorphous and microcrystalline structure. Hence, Ni-P/PZT/Ni-P composites with medium phosphorus content are able to achieve both high ME effect and low optimal magnetic field.

The flux concentration effect of high permeability materials provides a unique approach to developing highly sensitive magnetic field sensors. These small sized Ni-P/PZT/Ni-P cylindrical

laminates can be used for miniature devices and microelectronic circuits [17]. Moreover, the sensitivity can be further improved by using other piezoelectric materials as the PZT fiber to increase the piezoelectric voltage constant.

4. Conclusions

In summary, the Ni-P(Ni)/PZT/Ni-P(Ni) cylindrical layered ME composites with three different phosphorus contents of 0%, 9.78%

and 11.36%, have been obtained by electrodeposition and electroless deposition. In the Ni-P/PZT/Ni-P composites with 9.78% P, the curve of $\alpha_{E,A}$ dependence on the bias magnetic field, H_{DC} , exhibits the lowest $H_{dc,opt}$ and the best linearity compared with the other two samples. Besides, this composite also has a better comprehensive ME performance, namely, not only facilitating the ME devices miniaturization, but also expanding the magnetic field detection range at both low and high magnetic fields.

Acknowledgments

This work was supported by the Beijing Nova Program (Z141103001814006), by the National Key Technology R&D Program (Nos. 2012BAC12B05 and 2012BAC02B01), by the National Natural Science Foundation of China (Nos. 51174247 and U1360202), by the National High-Tech Research and the Development Program of China (No. 2012AA063202).

References

- [1] Ma J, Hu J, Li Z, et al. *Adv Mater* 2011;23:1062–87.
- [2] Vopsaroiu M, Cain MG, Sreenivasulu G, et al. *Mater Lett* 2012;66:282–4.
- [3] Bibes M, Barthélémy A. *Nat Mater* 2008;7:425–6.
- [4] Nan CW, Bichurin MI, Dong SX, et al. *J Appl Phys* 2008;103:031101–35.
- [5] Dong SX, Li JF, Viehland D. *Appl Phys Lett* 2004;85:5305–6.
- [6] Giang DTH, Quynh LK, Nghi NH, et al. *J Phys: Conf Ser* 2009;187:012057–5.
- [7] Pan DA, Bai Y, Volinsky AA, et al. *Appl Phys Lett* 2008;92:052904–3.
- [8] Pan DA, Bai Y, Chu WY, et al. *J Phys D: Appl Phys* 2008;41:022002–4.
- [9] Bi K, Wu W, Gu QL, et al. *J Alloys Compd* 2011;509:5163–6.
- [10] Zhai JY, Xing ZP, Dong SX, et al. *Appl Phys Lett* 2006;88:062510–3.
- [11] Dong SX, Zhai JY, Li JF, et al. *Appl Phys Lett* 2006;89:122903–3.
- [12] Zhai JY, Dong SX, Xing ZP, et al. *Appl Phys Lett* 2006;89:083507–3.
- [13] Pan DA, Wang J, Zuo ZJ, et al. *Appl Phys Lett* 2014;104:122903–4.
- [14] Li XS, Wang JB, Du LH. *Electroplat Pollut Control* 2007;27:20–2.
- [15] Bichurin MI, Filippov DA, Petrov VM, et al. *Phys Rev B* 2003;68:132408–4.
- [16] Hong H, Bi K, Wang YG. *J Alloys Compd* 2012;545:182–5.
- [17] Fang Z, Lu SG, Li F, et al. *Appl Phys Lett* 2009;95:112903–3.
- [18] Cao YQ, Yu HY, Zhao HJ, et al. *J Funct Mater* 2010;41:296–9.
- [19] Jiang TX, Wu HH. *Chem J Chin Univ* 2001;22:976–9.